Article

Cell Reports

Ligand-Occupied Integrin Internalization Links Nutrient Signaling to Invasive Migration

Graphical Abstract

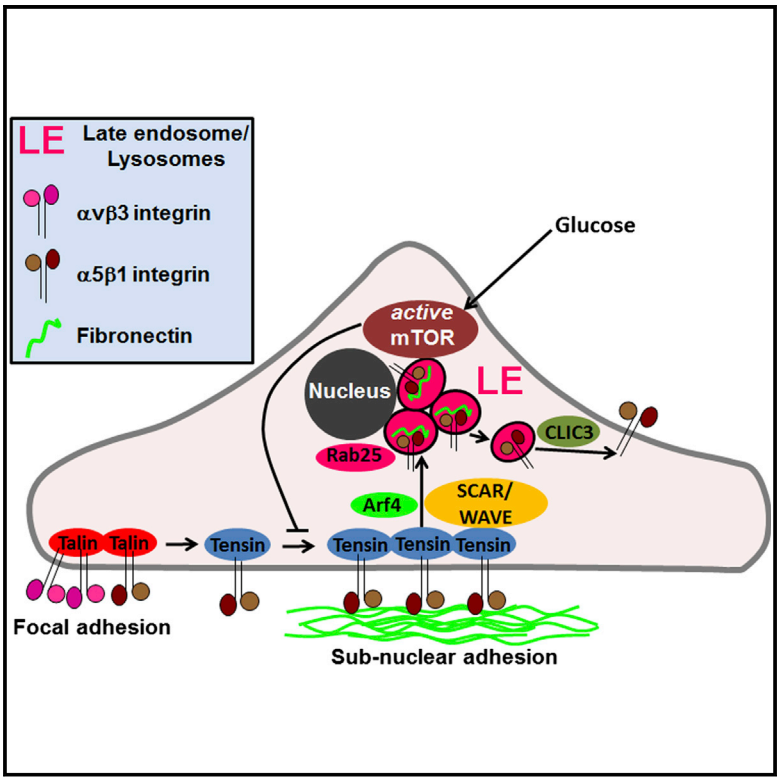

Authors

Elena Rainero, Jonathan D. Howe, ..., Laura Machesky, Jim C. Norman

Correspondence

j.norman@beatson.gla.ac.uk

In Brief

Rainero et al. find that α5β1 integrins are first moved from the cell periphery to a region beneath the nucleus and from here are endocytosed and trafficked to late endosomes to support mTOR signaling. Control of this proinvasive pathway by nutrient status provides evidence for mechanistic links among ECM internalization, nutrient signaling, and metastasis.

Highlights

- Tensin positions integrins for Arf4-dependent endocytosis
- Photoactivation-in-TIRF microscopy pinpoints the site for integrin endocytosis
- Integrin endocytosis dictates recruitment of mTORC1 to nearby late endosomes
- Proinvasive trafficking pathway is regulated by nutrient status

Rainero et al., 2015, Cell Reports *10*, 398–413
January 20, 2015
http://dx.doi.org/10.1016/j.celrep.2014.12.037

OPEN ACCESS
CellPress

Cell Reports
Article

Ligand-Occupied Integrin Internalization Links Nutrient Signaling to Invasive Migration

Elena Rainero,[1] Jonathan D. Howe,[2,3] Patrick T. Caswell,[1,4] Nigel B. Jamieson,[5] Kurt Anderson,[1] David R. Critchley,[2] Laura Machesky,[1] and Jim C. Norman[1,*]

[1]Beatson Institute for Cancer Research, Garscube Estate, Glasgow G61 1BD, UK
[2]Department of Biochemistry, University of Leicester, Leicester LE1 7RH, UK
[3]Cell Biology Division, MRC Laboratory of Molecular Biology, Francis Crick Avenue, Cambridge Biomedical Campus, Cambridge CB2 0QH, UK
[4]Cell-Matrix Research, Faculty of Life Sciences, University of Manchester, Manchester M13 9PT, UK
[5]West of Scotland Pancreatic Unit, Glasgow Royal Infirmary, Alexandra Parade, Glasgow G31 2ER, UK
*Correspondence: j.norman@beatson.gla.ac.uk
http://dx.doi.org/10.1016/j.celrep.2014.12.037

SUMMARY

Integrin trafficking is key to cell migration, but little is known about the spatiotemporal organization of integrin endocytosis. Here, we show that α5β1 integrin undergoes tensin-dependent centripetal movement from the cell periphery to populate adhesions located under the nucleus. From here, ligand-engaged α5β1 integrins are internalized under control of the Arf subfamily GTPase, Arf4, and are trafficked to nearby late endosomes/lysosomes. Suppression of centripetal movement or Arf4-dependent endocytosis disrupts flow of ligand-bound integrins to late endosomes/lysosomes and their degradation within this compartment. Arf4-dependent integrin internalization is required for proper lysosome positioning and for recruitment and activation of mTOR at this cellular subcompartment. Furthermore, nutrient depletion promotes subnuclear accumulation and endocytosis of ligand-engaged α5β1 integrins via inhibition of mTORC1. This two-way regulatory interaction between mTORC1 and integrin trafficking in combination with data describing a role for tensin in invasive cell migration indicate interesting links between nutrient signaling and metastasis.

INTRODUCTION

The cell's major fibronectin-binding integrin (α5β1) promotes survival and migration of tumor cells (Caswell et al., 2008; Lee and Juliano, 2000), making this an important molecule for cell biologists interested in cancer progression. α5β1 integrin is continuously internalized, trafficked to recycling endosomes and then returned, or recycled, to the plasma membrane via both Rab11- and Arf6-dependent pathways (Caswell and Norman, 2006; Pellinen and Ivaska, 2006). However, α5β1 integrins that are ligand-engaged do not reach recycling endosomes but are sent to lysosomes under control of Rab25 (Dozynkiewicz et al., 2012; Lobert et al., 2010; Rainero and Norman, 2013). Moreover, Rab25 expression is associated with upregulation of a lysosomal protein called CLIC3, which prevents degradation of α5β1 and allows recycling from this compartment to the plasma membrane (Dozynkiewicz et al., 2012).

Membrane trafficking pathways influence α5β1's capacity to promote invasion. Expression of mutant p53s promote association of Rab-coupling protein (RCP) with α5β1, which then associates with receptor tyrosine kinases (RTKs) to promote invasion (Caswell et al., 2008; Muller et al., 2009, 2012). Conversely, when α5β1 is trafficked to late endosomes and lysosomes, this is associated with invasion and metastasis, but via activation of c-Src (Dozynkiewicz et al., 2012; Lobert and Stenmark, 2012).

β1 integrins follow endocytic routes that depend on clathrin (Ezratty et al., 2009; Pellinen et al., 2008; Teckchandani et al., 2009), caveolin (Shi and Sottile, 2008), macropinocytosis (Gu et al., 2011), and clathrin-independent carriers (Howes et al., 2010). However, it is currently unclear what dictates which endocytic route will be taken by a given heterodimer. Spatially distinct pools of β1 integrins may follow different endocytic pathways. Endocytosis mediated by the unconventional clathrin adaptor, Dab2, is thought to occur at the cell's upper surface (Teckchandani et al., 2009). But, reports indicating that unconventional clathrin adaptors mediate internalization of integrins from focal adhesions underneath the cell indicate that this situation is far from clear (Chao and Kunz, 2009; Ezratty et al., 2009).

Ligand-engaged integrins are routed to late endosomes/lysosomes, and studies looking at trafficking of internalized conformation-specific anti-integrin antibodies show that these traffic with different kinetics (Arjonen et al., 2012). The canonical view is that all endocytic traffic converges on early endosomes despite the route taken into the cell. However, membrane components can enter endocytic compartments, such as lysosomes without passing through early endosomes (Lippincott-Schwartz and Fambrough, 1987). Taken together with reports indicating that integrins in different conformations are internalized via different mechanisms (Chao and Kunz, 2009; Valdembri et al., 2009) this suggests that, rather than entering the cell via the

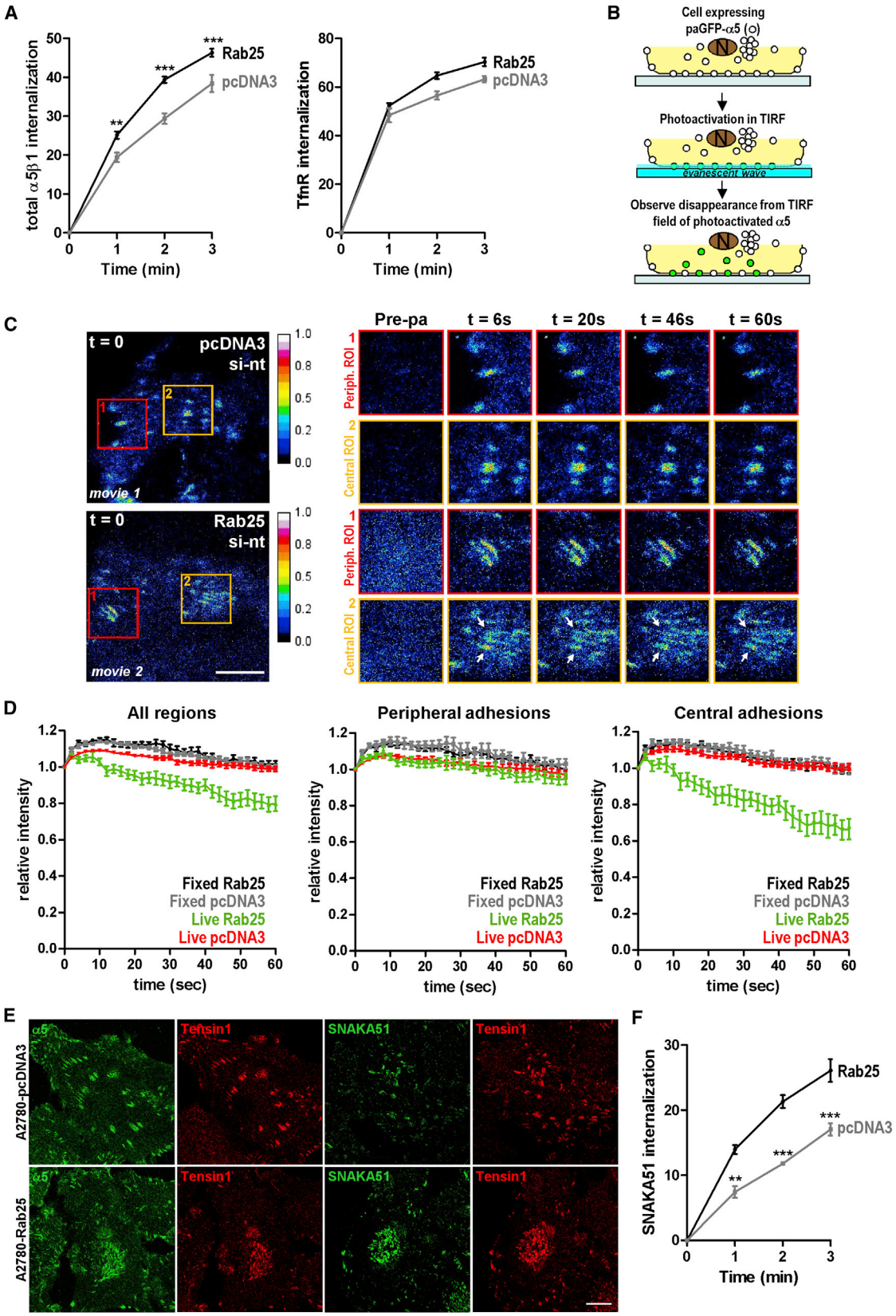

(legend on next page)

same route and then being triaged in early endosomes, the internal destination of integrin conformers may be dictated by the route used to enter the cell in the first place.

We have developed approaches to closely define the spatial organization of α5β1 endocytosis, and how this influences its subsequent intracellular trafficking. We find that in Rab25-expressing cells α5β1 associates with tensin to be transported centripetally from the cell periphery to a region under the nucleus. From here, an Arf4-dependent internalization pathway channels integrin and extracellular matrix (ECM) proteins to late endosomes/lysosomes. Integrin flow through this pathway is necessary to maintain a population of centrally located late endosomes/lysosomes capable of recruiting and activating mTOR. This spatially restricted trafficking of a particular subpopulation of integrins between fibrillar adhesions and lysosomes provides evidence for mechanistic links between ECM internalization, nutrient signaling, and the progression of cancer.

RESULTS

Activated Integrins Are Endocytosed at Centrally Located Adhesions in Rab25-Expressing Cells

We measured α5β1 endocytosis using capture-ELISA (Roberts et al., 2001) in the presence of the receptor recycling inhibitor, primaquine, to ensure that estimates of integrin endocytosis were not affected by recycling. α5β1 was rapidly internalized by A2780 ovarian cancer cells, and this was modestly enhanced by Rab25 expression, whereas endocytosis of transferrin receptor (TfnR) was unaffected (Figure 1A). To directly visualize integrin endocytosis and determine its spatial characteristics, we combined photoactivation with total internal reflection fluorescence (TIRF) microscopy. We expressed photoactivatable GFP-α5 (paGFP-α5) in A2780 cells and activated it using a pulse of 405 nm laser light restricted by TIRF to ensure that only receptors present at the cell surface were illuminated (Figure 1B). Having established the kinetics of photoactivation/photobleaching in paraformaldehyde-fixed cells (Figure 1D), we found that, in living cells, Rab25 promoted a modest (but significant) increase in internalization of photoactivated α5β1 from the TIRF field (Figures 1C and 1D; Movies S1 and S2). Moreover, quantitative analyses of TIRF movies indicated that, in Rab25-expressing cells, paGFP-α5 left the TIRF field more quickly from adhesions that were centrally located than from the cell periphery (Figures 1C and 1D).

Although many adhesion components (αvβ3, talin, and vinculin) reside within focal adhesions, α5β1 and tensin translocate from these to populate more centrally located fibrillar adhesions (Pankov et al., 2000). To look at fibrillar adhesion morphology more closely, we plated control and Rab25-expressing A2780 cells onto fibronectin-coated surfaces and used confocal microscopy to visualize tensin and α5β1. Rab25 drove accumulation of α5β1 and tensin-rich adhesions at a well-defined patch directly under the nucleus (Figure 1E). SNAKA51, an antibody that recognizes a conformation of activated α5β1 enriched in fibrillar adhesions (Clark et al., 2005), preferentially stained centrally located tensin-rich adhesions in Rab25-expressing cells (Figure 1E). Rab25-expressing cells internalized SNAKA51-conformation α5β1 at least 2-fold faster than control A2780 cells (Figure 1F) which, in combination with the photoactivation data, indicates that Rab25 increases endocytosis of integrins from centrally located fibrillar adhesions.

We constructed a photoactivatable tensin-1 (paGFP-tensin-1) and investigated the rate at which this leaves adhesions. Photoactivated tensin left the TIRF field much more slowly than did α5β1, and this was not affected by Rab25 expression (Figure S1A), indicating that the rate at which integrin leaves centrally located adhesions to follow an endocytic route exceeds the rate at which the adhesive structure itself is turned over.

Tensin Controls Centripetal Movement to Centrally Position Integrins for Endocytosis

Our observations that α5β1 integrin endocytosis occurs from the central, subnuclear region suggested that centripetal movement from the cell periphery might be a prerequisite for integrins to enter the cell via this route. We used a modification of the approach described by Pankov et al. (2000) to quantify the rate at which α5β1-containing adhesions translocate away from the cell periphery following plating onto fibronectin-coated surfaces.

Figure 1. α5β1 Is Internalized at Centrally Located Fibrillar Adhesions

(A) A2780 cells expressing Rab25 or control vector (pcDNA3) were surface-labeled with 0.13 mg/ml NHS-S-S-Biotin at 4°C and internalization allowed to proceed at 37°C for the indicated times in the presence of 0.6 mM primaquine. Biotin remaining at the cell surface was removed by exposure to MesNa at 4°C, and the quantity of biotinylated receptors within the cells was determined by capture-ELISA using microtiter wells coated with monoclonal antibodies recognizing α5 (clone VC5) or TfnR. Values are mean ± SEM from three independent experiments; $^{**}p < 0.01$, $^{***}p < 0.001$; ANOVA test.

(B) Schematic representation of photoactivation-in-TIRF. Photoactivatable GFP-α5 (paGFP-α5) -expressing cells were plated onto fibronectin-coated glass coverslips. Evanescent field illumination at 405 nm is used to selectively photoactivate paGFP-α5 within ≈150 nm of the coverslip surface. The subsequent loss of photoactivated integrin from the plasma membrane is then observed using TIRF microscopy.

(C and D) A2780-pcDNA3 and A2780-Rab25 cells were transfected with paGFP-α5 and farnesylated-Cherry (to enable visualization of cells prior to photoactivation) in combination with nontargeting siRNA (si-nt) and allowed to attach to glass dishes coated with fibronectin (25 μg/ml) for 16 hr. paGFP-α5 was photoactivated with a pulse of 405 nm laser light via evanescent field illumination (as in B), and TIRF movies were captured with 2 s frame intervals over a period of 60 s. A prephotoactivation image (Pre-pa) and five further time points from regions of interest (ROI) at the cell periphery (red boxes; #1) and central region (yellow boxes; #2) of this sequence (0, 6, 20, 46, and 60 s) are shown. The stills in (C) are extracted from Movies S1 and S2. Scale bar, 16 μm. The fluorescence intensity of adhesions from all regions (D; left graph) of the cell bottom, and those within peripheral (D; central graph) or central (D; right graph) ROIs were determined. To determine the kinetics of photoactivation and photobleaching, cells were fixed with paraformaldehyde prior to photoactivation as indicated. Values are mean ± SEM; number of cells, 28 (fixed Rab25), 29 (fixed pcDNA3), 34 (live Rab25), and 40 (live pcDNA3).

(E) A2780-pcDNA3 and A2780-Rab25 cells were plated onto glass dishes coated with fibronectin (25 μg/ml) for 16 hr and then fixed, and α5 integrin (left panels, clone VC5; right panels clone SNAKA51) and tensin-1 were visualized by immunofluorescence followed by confocal microscopy. Scale bar, 20 μm.

(F) The graph displays internalization of α5 integrin determined as for (A), but with the SNAKA51 antibody used for detection of biotinylated integrin in the capture-ELISA. Values are mean ± SEM from three independent experiments; $^{**}p < 0.01$, $^{***}p < 0.001$; ANOVA test.

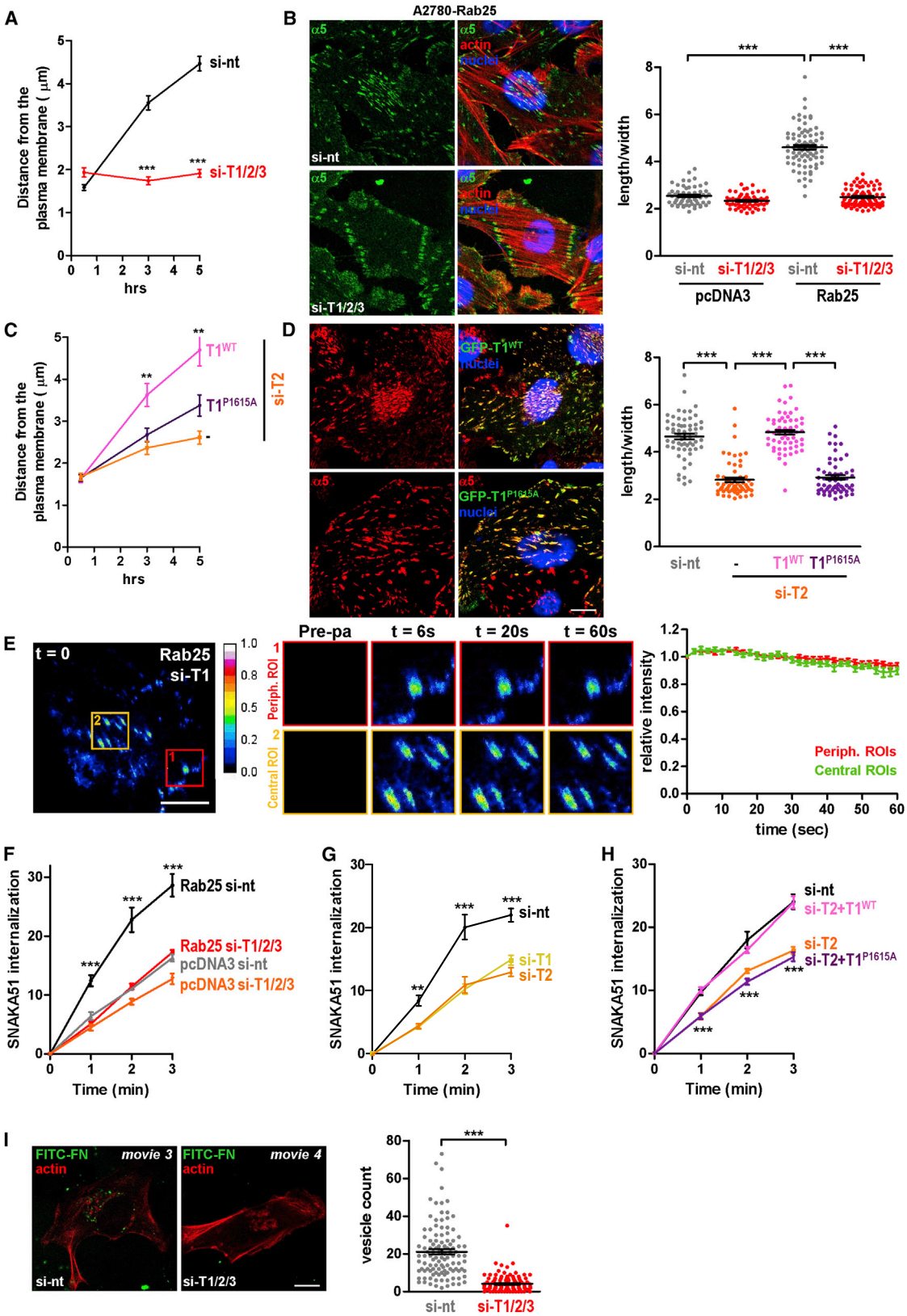

(legend on next page)

Shortly following cell attachment, α5β1-adhesions were located close (<2μm) to the cell periphery, and these translocated centripetally to populate the central region of the cell (>4μm from the cell periphery) over the ensuing 5 hr (Figure 2A; Figure S1B). When α5β1 integrins move centripetally they part company with focal adhesion components, such as talin and vinculin, but are thought to maintain association with tensin, and experiments in which the actin homology 2 domain of tensin was overexpressed had previously suggested a possible role for tensin in integrin translocation to the cell center (Pankov et al., 2000). Combined small interfering RNA (siRNA) of tensins-1, -2, and -3 (Figure 2A; Figures S1B and S1C) or knockdown of an individual tensin (Tensin-2; Figure 2C) significantly opposed movement of α5β1 from the cell periphery toward the subnuclear region. Furthermore, α5β1-containing adhesions in tensin-knockdown A2780-Rab25 cells were not only more peripheral but had reduced length/width ratio indicating that they were less fibrillar (Figure 2B).

Tensin binds to β1 integrins via an interaction between tensin's PTB-like domain and the membrane proximal NPxY motif of the β1 integrin cytotail, and we have recently shown that β1 integrins with mutations in this motif are not efficiently endocytosed (Margadant et al., 2012). The structural requirements for tensin-integrin association have been studied in detail (McCleverty et al., 2007). Informed by these studies, we constructed a GFP-tagged mutant of tensin, GFP-tensin^{Pro1615Ala}, that is unable to associate with β1 integrin and investigated its ability to support centripetal movement of α5β1 in Rab25-expressing cells. Although expression of wild-type GFP-tensin restored centripetal movement of α5β1 (Figure 2C) and fibrillar adhesion morphology (Figure 2D) in tensin knockdown cells, GFP-tensin^{Pro1615Ala} was significantly less effective in both of these regards.

Photoactivation-in-TIRF indicated that most α5β1 endocytosis occurs from the central/subnuclear region of the cell. Given that we have found tensin to be required for movement of α5β1 into this region, we anticipated that integrin endocytosis might be impaired in tensin knockdown cells. Photoactivated α5β1 did not leave the TIRF field from either peripheral or central regions following siRNA of tensin (Figure 2E). Consistently, knockdown of tensins-1, -2, and -3, either alone or in combination (Figures 2F and 2G), strongly suppressed internalization of SNAKA51-conformation α5β1 integrins (but not TfnR [Figure S1D]) in Rab25-expressing cells, whereas endocytosis in control A2780 cells was unaffected by tensin knockdown. Furthermore, whereas GFP-Tensin restored endocytosis of SNAKA51-conformation integrins in tensin knockdown cells, GFP-Tensin^{Pro1615Ala} was completely ineffective in this regard (Figure 2H).

Because SNAKA51 recognizes a ligand-bound conformation of α5β1, we plated A2780-Rab25 cells onto glass surfaces coated with fluorescein-conjugated fibronectin and used confocal microscopy to determine its endocytosis. Fluorescent fibronectin was transported into cytoplasmic vesicles that were visible above the plane of adhesion (Figure 2I; Movie S3). The number of fibronectin-positive intracellular vesicles was reduced by siRNA of tensins-1, -2, and -3 (Figure 2I; Movie S4), indicating that α5β1 heterodimers entering the cell via the tensin-dependent pathway are ligand bound.

In NIH 3T3 fibroblasts, the proportion of α5β1 integrin localized to tensin-positive fibrillar adhesions was much higher than for A2780-Rab25 cells (Figure S2A). We introduced siRNAs targeting mouse tensins-1 and -2 (Figure S2C) in NIH 3T3 fibroblasts and were unable to detect differences in the morphology of fibrillar adhesions (Figures S2A and S2B), consistent with previous studies indicating that tensins play little or no role in fibrillar adhesion assembly in fibroblasts (Clark et al., 2010). Photoactivated paGFP-α5 was rapidly lost from the TIRF field across the whole bottom surface of NIH 3T3 cells (Figure S2D), and internalization of α5β1 was strongly opposed by knockdown of tensins

Figure 2. Tensin-β1 Integrin Association Controls Centripetal Movement to Centrally Position α5β1 for Endocytosis

(A and B) A2780-pcDNA3 and A2780-Rab25 cells were transfected with siRNAs targeting tensins-1, -2, and -3 (si-T1/2/3) or nontargeting control (si-nt). Cells were plated onto glass dishes coated with fibronectin (25 μg/ml) for 30 min, 3 and 5 hr (A), or for 16 hr (B) and then fixed and stained for α5 integrin using the VC5 antibody and counterstained with DAPI and phalloidin to visualize nuclei and F-actin. Scale bar, 20 μm. Centripetal movement (quantified by measuring the distance between α5-positive adhesions and the closest plasma membrane at the indicated times following initiation of cell spreading) (A) and the geometry (B) of endogenous α5-containing adhesions was determined using ImageJ. The mean and SEM from three independent experiments are indicated; ***p < 0.001; ANOVA test.

(C and D) A2780-Rab25 cells were transfected with siRNAs targeting tensin-2 in combination with GFP-tensin-1^{WT} (GFP-T1^{WT}) or GFP-tensin-1^{P1615A} (GFP-T1^{P1615A}) and centripetal movement (C) and adhesion morphology (B) quantified. Mean and SEM from three independent experiments are indicated; ***p < 0.001; ANOVA test.

(E) A2780-Rab25 cells were transfected with an siRNA targeting tensin-1 (si-T1) in combination with paGFP-α5, and internalization from the TIRF field following photoactivation was determined as for Figures 1C and 1D. ROI at the cell periphery (red box; #1) and central region (yellow box; #2) are displayed as stills and quantified as for Figure 1D. The siRNA controls that correspond to these experiments are displayed in Figures 1C and 1D. Values are mean ± SEM, number of cells = 30.

(F and G) A2780-pcDNA3 and A2780-Rab25 cells were transfected with siRNAs targeting tensins-1, -2, and -3 (si-T1/2/3) or nontargeting control (si-nt), and internalization of SNAKA51-conformation α5β1 determined as for Figure 1F. Values are mean ± SEM from three independent experiments. **p < 0.01, ***p < 0.001; ANOVA test.

(H) A2780-Rab25 cells were transfected with siRNAs targeting tensin-2 in combination with GFP-tensin-1^{WT} (GFP-T1^{WT}) or GFP-tensin-1^{P1615A} (GFP-T1^{P1615A}), and internalization of SNAKA51-conformation α5β1 was determined as for (F). Values are mean ± SEM from three independent experiments. ***p < 0.001; ANOVA test

(I) A2780-Rab25 cells were transfected with siRNAs targeting tensins-1, -2, and -3 (si-T1/2/3) or nontargeting control (si-nt) in the presence of life-Act (red) and plated onto glass dishes coated with fluorescein-labeled fibronectin (FITC-FN; 25 μg/ml). Uptake of FITC-FN (green) into living cells was visualized by fluorescence confocal video microscopy with the plane of focus situated in the plane of the nucleus (see Movies S3 and S4). The quantity of vesicles containing FITC-FN were quantified. The mean and SEM from three independent experiments are indicated; ***p < 0.001; Mann-Whitney test.

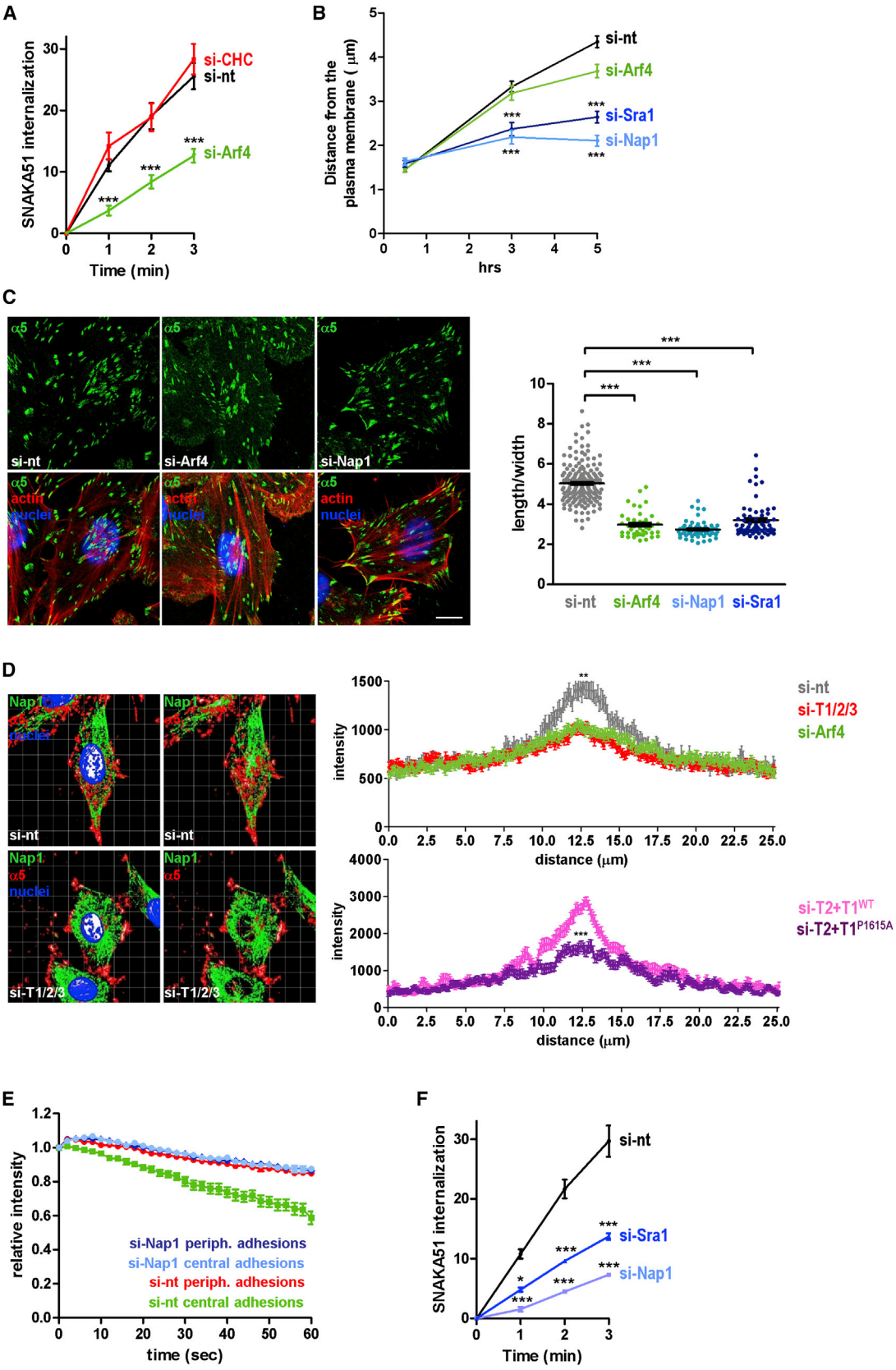

(legend on next page)

irrespective of whether we used photoactivation-in-TIRF (Figure S2D) or capture-ELISA (Figure S2E) to measure this. Moreover, the capture-ELISA gave similar results whether SNAKA51 or an antibody recognizing all conformations of α5β1 was used as the capture antibody (Figure S2E). Thus, in Rab25-expressing A2780 cells, tensin and its association with theβ1 integrin cytodomain are required for both the centripetal movement of integrins to the subnuclear zone and subsequent internalization of ligand-bound α5β1 from this region. In fibroblasts, which incorporate a much higher proportion of their α5β1 into fibrillar-type adhesions, tensins are essential for endocytosis of α5β1 despite playing no role in assembly of these structures.

Arf4 Is Required for Internalization of Ligand-Engaged α5β1

Given the reported role of clathrin in integrin internalization, it was surprising that siRNA of clathrin (Figure S3A) did not suppress α5β1 endocytosis irrespective of the antibody used for the capture-ELISA (Figure 3A; data not shown), nor did it affect the morphology of α5β1 adhesions (data not shown). Furthermore, we have been unable to detect any reduction of α5β1 endocytosis in A2780 cells or in NIH 3T3 fibroblasts following treatment with drugs, such as Dynasore or monodansylcadaverine, that interfere with clathrin-dependent endocytosis (data not shown). The Arf subfamily of GTPases has three subclasses: class I (Arfs 1, 2, and 3); class II (Arfs 4 and 5); and class III (Arf6). Although class I and III Arfs have established roles in endocytosis and recycling (D'Souza-Schorey and Chavrier, 2006;Kumari and Mayor, 2008), less is known about the function of class II Arfs. Indications from mass spectrometry screens suggested that Arf4 might be weakly associated with immunoprecipitated tensin (data not shown), and we therefore investigated whether this class II Arf participates in α5β1 endocytosis. siRNA of Arf4 (Figure S3A) did not oppose centripetal movement of α5β1 from the cell periphery to the subnuclear zone in A2780-Rab25 cells (Figure 3B). However, Arf4 knockdown strongly suppressed endocytosis of SNAKA51-conformation α5β1 integrins (but not TfnR [Figure S3B]) in A2780-Rab25 cells and in NIH 3T3 fibroblasts (Figure 3A;Figures S2F and S2G). Consistent with these observations, siRNA of Arf4 led to accumulation of bulky α5β1-containing adhesions under the central region of A2780-Rab25 cells (Figure 3C).

Role of the SCAR/WAVE Complex in Centripetal Movement and Endocytosis of α5β1

Tensin is an actin-binding protein, so we investigated whether an actin-dependent mechanism is involved in centripetal movement and internalization of α5β1 in A2780-Rab25 cells. Key to control of cellular actin dynamics is the SCAR/WAVE complex, which consists of a number of core subunits (such as Nap1 and Sra1), which promote Arp2/3-dependent nucleation of actin filaments (Tang et al., 2013). Quantitative immunofluorescence indicated that, in A2780-Rab25 cells, SCAR/WAVE was concentrated under the nucleus, in close association with the tensin-positive centrally located adhesions, and that SCAR/WAVE positioning was opposed by siRNA of Arf4 or disruption of tensin-integrin association (Figure 3D). Consistently, siRNA of SCAR/WAVE subunits Nap-1 or Sra1 strongly opposed centripetal movement of α5β1 to the subnuclear region (Figure 3B) and endocytosis of photoactivated paGFP-α5 integrin from this zone (Figure 3E). Moreover, capture-ELISA indicated that SCAR/WAVE was required for endocytosis of ligand-engaged α5β1 in both A2780-Rab25 cells (Figure 3F) and NIH 3T3 fibroblasts (Figure S2F).

Late Endosomes/Lysosomes Visit Tensin-Positive Adhesions under Control of Arf4

In Rab25-expressing cells, ≈80% of late endosomes/lysosomes were located in the cell's central region in close apposition to centrally located adhesions (Figures 4A and 4B). Consistently, in Rab25-expressing (but not control) A2780 cells the central positioning of late endosomes/lysosomes depended on the fibronectin concentration used to coat the substratum (Figure 4B; Figure S4A), and this correlated closely with assembly of subnuclear adhesions (Figure S4A). Importantly, central positioning of lysosomes was significantly reduced by siRNA of either tensins or Arf4 (Figure 4B; Figure S4B). Similarly, in NIH 3T3 fibroblasts congregation of lysosomes under the nucleus was dependent on the fibronectin-coating concentration and was opposed by knockdown of tensin (Figure S5A).

Analysis of TIRF movies indicated that mCherry-Rab25-positive late endosomes (but not recycling [Rab11] or early [Rab4] endosomes) made frequent and persistent contacts with GFP-Tensin-1 and GFP-Tensin-2-positive fibrillar adhesions (Figure S4C). The same was seen when GFP-α5 was used to mark fibrillar adhesions and LAMP1-cherry to visualize late

Figure 3. Arf4 and the SCAR/WAVE Complex Are Required for Internalization of Ligand-Engaged α5β1

(A) A2780-Rab25 cells were transfected with siRNAs targeting clathrin heavy chain (si-CHC), Arf4 (si-Arf4), or nontargeting control (si-nt) and internalization of SNAKA51-conformation α5β1 determined as for Figure 1F. Values are mean ± SEM from three independent experiments; ***$p < 0.001$; ANOVA test.

(B and C) A2780-Rab25 cells were transfected with siRNAs targeting Arf4 (si-Arf4), Nap1 (si-Nap1), Sra1 (si-Sra1), or nontargeting control (si-nt), plated onto glass-bottom dishes coated with fibronectin (25 μg/ml), for 30 min, 3 or 5 hr (B), or for 16 hr (C) and then fixed and stained for α5 integrin using the VC5 antibody and counterstained with DAPI and phalloidin to visualize nuclei and F-actin. Scale bar, 20 μm. Centripetal movement (B) and the geometry (C) of endogenous α5 containing adhesions was determined as for Figure 2. The mean and SEM from three independent experiments are indicated; ***$p < 0.001$; ANOVA test.

(D) A2780-Rab25 cells were transfected with siRNAs targeting tensins-1, -2, and -3 (si-T1/2/3), Arf4 (si-Arf4) or nontargeting control (si-nt), or with siRNAs targeting tensin-2 in combination with GFP-tensin-1^{WT} (GFP-$T1^{WT}$) or GFP-tensin-1^{P1615A} (GFP-$T1^{P1615A}$), plated onto glass-bottom dishes coated with fibronectin (25 μg/ml), for 16 hr, and then fixed and stained for Nap1 and α5 integrin, and counterstained with DAPI to visualize nuclei. z stacks of confocal images were collected and assembled into a 3D reconstruction using Volocity software. Line-scan analysis was performed using ImageJ. **$p < 0.01$, ***$p < 0.001$; ANOVA test.

(E and F) A2780-Rab25 cells were transfected with siRNAs targeting Nap1 (si-Nap1), Sra1 (si-Sra1), or nontargeting control (si-nt) in combination with paGFP-α5 (E) and plated onto glass-bottom dishes coated with fibronectin (25 μg/ml) (E) or on plastic surfaces (F). Internalization from the TIRF field following photoactivation was determined as for Figures 1C and 1D. Internalization of SNAKA51-conformation α5β1 was determined as for Figure 1F. The mean and SEM from three independent experiments are indicated; ***$p < 0.001$, *$p < 0.05$; ANOVA test.

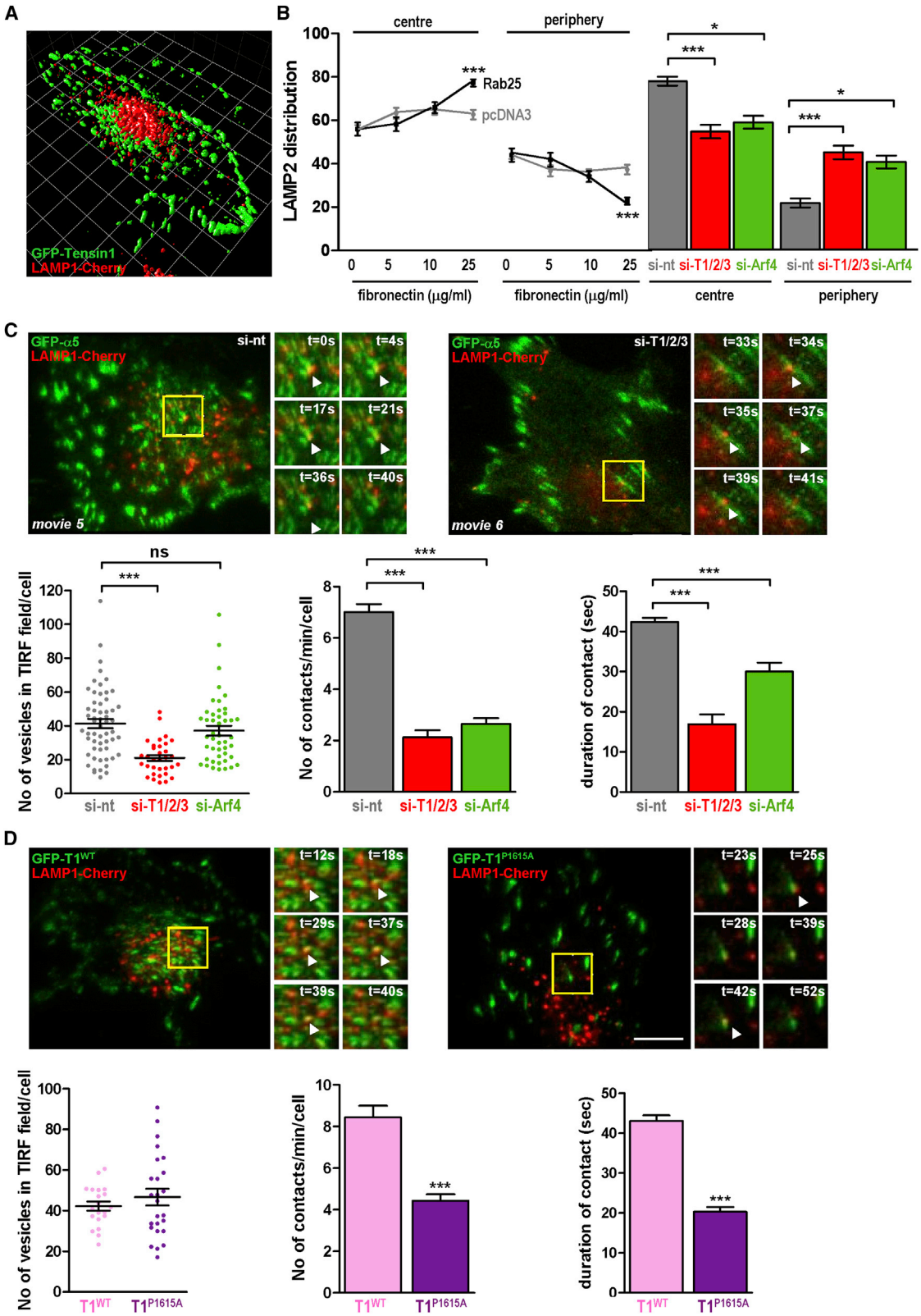

(legend on next page)

endosomes (Figure 4C; Movie S5), and it was possible to see the arrival of late endosomes coinciding with adhesion disassembly and concomitant appearance of GFP-α5 within the endosome (Movie S5). Consistently, in NIH 3T3 fibroblasts late endosomes/lysosomes (but not early endosomes) regularly contacted GFP-tensin-1 adhesions (Figure S5B). Importantly, a range of measures that we have found to oppose integrin centripetal movement and/or internalization of ligand-engaged integrins (for example, siRNA of tensins or Arf4 and ablation of integrin-tensin association using GFP-Tensin^{Pro1615Ala}) significantly reduced the number and duration of contacts between fibrillar adhesions and late endosomes (Figures 4C and 4D).

The Tensin/Arf4 Internalization Pathway Targets α5β1 to Lysosomes

Internalized α5β1 colocalized with LAMP1, EEA1, and Rab11 indicating that integrins are trafficked to early and recycling endosomes and late endosomes/lysosomes (Figure 5A). Moreover, active integrins were abundant in late endosomes/lysosomes as detected with the 9EG7 antibody, which recognizes an extended conformation of active β1 integrin (Figure 5B). By contrast, active β1 integrins were not abundant in early endosomes (Figure 5C). Delivery of α5β1 to LAMP1-positive compartments was reduced by knockdown of tensin or Arf4 (Figures 5A and 5B). By contrast, the fraction of α5β1 trafficked to recycling endosomes was unaffected by tensin knockdown, and the amount of integrin sent to early endosomes was significantly increased (Figure 5A). Taken together, these data indicate that tensin and Arf4 promote transit of α5β1 from fibrillar adhesions to late endosomes without passage through EEA1 or Rab11-positive compartments.

We determined whether endocytic delivery of α5β1 to lysosomes is linked to its degradation. In the presence of fibronectin to increase the quantity of active integrin, internalized α5β1 was degraded over a period of a few hours (in CLIC3 knockdown A2780 cells, and in NIH 3T3 fibroblasts), and this was strongly opposed by tensin knockdown (Figure 5D).

Tensin and Arf4 Control Lysosomal Recruitment and Activation of mTOR

Nutrient availability is a requirement for mTORC1 activation, and mTOR recruitment to late endosomal/lysosomal compartments is integral to this (Efeyan et al., 2012). Lysosomal positioning can influence mTORC1 (Korolchuk et al., 2011), prompting us to investigate a possible relationship between α5β1 internalization and lysosomal recruitment and activity of mTOR. Rab25-expressing cells had significantly increased levels of phosphorylated 4EBP1 (an mTORC1 substrate) and enhanced recruitment of mTOR to CD63-positive late endosomes/lysosomes by comparison with control A2780 cells (Figures 6A and 6B). Interestingly, other signaling events downstream of mTOR (such as phosphorylation of ribosomal S6 protein, Akt, and ULK1) were not enhanced by expression of Rab25, indicating that lysosomal recruitment of mTOR may play a particular role in maintenance of 4EBP1 phosphorylation. In A2780-Rab25 cells, siRNA of tensins or Arf4 opposed mTOR recruitment to lysosomes (Figure 6B), and levels of phospho-4EBP1 were significantly reduced by knockdown of tensin, Arf4, or Nap1 (Figures 6A and S6A). Consistently, in NIH 3T3 fibroblasts lysosomal recruitment of mTOR was opposed by siRNA of tensin (Figure S6B).

Control of α5β1 Endocytosis by Glucose and mTORC1

Cells are thought to respond to starvation by upregulating processes that lead to nutrient uptake. We tested whether starvation could influence integrin endocytosis and found that removal of glucose from the medium constitutes a powerful stimulus to assembly of subnuclear adhesions (Figure S7A) and to internalization of SNAKA51-conformation α5β1 in A2780 cells (Figure 6C). As glucose depletion leads to substantial reduction of mTORC1 activity in A2780 cells (Figure S7B), we determined whether mTORC1 inhibition would influence internalization of ligand-engaged α5β1. We inhibited mTORC1 by treating A2780 cells with Rapamycin or by knocking down the mTORC1 component, Raptor, and both of these manipulations promoted internalization of SNAKA51-conformation α5β1 (but not TfnR) (Figures 6D, 6E, S7C, and S7D). Conversely, knockdown of the essential mTORC2 component, Rictor, had no effect on integrin endocytosis in A2780 cells. These data indicate that mimicking nutrient starvation by inhibiting mTORC1 promotes translocation of α5β1 into fibrillar adhesions (Figure S7A) and endocytosis of ligand-bound integrins from these structures, whereas mTORC2 does not contribute to these processes.

Figure 4. Late Endosomes/Lysosomes Visit Tensin-Positive Adhesions under Control of Arf4

(A) A2780-Rab25 cells were transfected with GFP-tensin1 (green) and LAMP1-cherry (red) and allowed to adhere to glass-bottomed dishes coated with fibronectin (25 μg/ml) for 16 hr. Cells were fixed and z stacks of confocal images were collected and assembled into a 3D reconstruction using Volocity software. In this 45° angle projection, the close apposition of late endosomes and centrally located fibrillar adhesions can be clearly seen.

(B) A2780-pcDNA3 and A2780-Rab25 cells were transfected with siRNAs targeting tensins-1, -2, and -3 (si-T1/2/3), Arf4 (si-Arf4) or nontargeting control (si-nt) and allowed to attach for 16 hr to glass dishes that were precoated with either 25 μg/ml fibronectin or the indicated concentrations of fibronectin. Cells were imaged by confocal microscopy, and the distribution of LAMP2 in a confocal section corresponding to the plane of adhesion was determined using a macro (see Figure S4B) that describes regions running progressively from the cell edge to the cell center and determines the proportion of LAMP2 that was present either <4 μm (periphery) or >4 μm (center) from the cell edge. Values are mean ± SEM from three independent experiments; *$p < 0.05$, ***$p < 0.001$; ANOVA test.

(C) A2780-Rab25 cells were transfected with GFP-α5 (green) and LAMP1-cherry (red) in combination siRNAs targeting tensins-1, -2, and -3 (si-T1/2/3) or nontargeting control (si-nt) and allowed to adhere as for (A). TIRF movies were captured with 0.5 s frame intervals over a period of 60 s. Time points from a region of interest (yellow box) in the cell's central region are shown. The stills are extracted from Movies S5 and S6. Scale bar, 16 μm. The quantity of LAMP1-positive vesicles visible within the TIRF field were determined using ImageJ (left graph). The number and duration of contact events between GFP-α5-positive structures and LAMP1-cherry vesicles were quantified and are presented as histograms. The mean and SEM from three independent experiments are indicated; ***$p < 0.001$; ANOVA test.

(D) A2780-Rab25 cells were transfected with siRNAs targeting tensin-2 in combination with LAMP1-cherry (red) and GFP-tensin-1^{WT} or GFP-tensin-1^{P1615A} (green). Cells were allowed to adhere and TIRF movies were captured and quantified as in (C). Bar, 16 μm. The mean and SEM from three independent experiments are indicated; ***$p < 0.001$; ANOVA test.

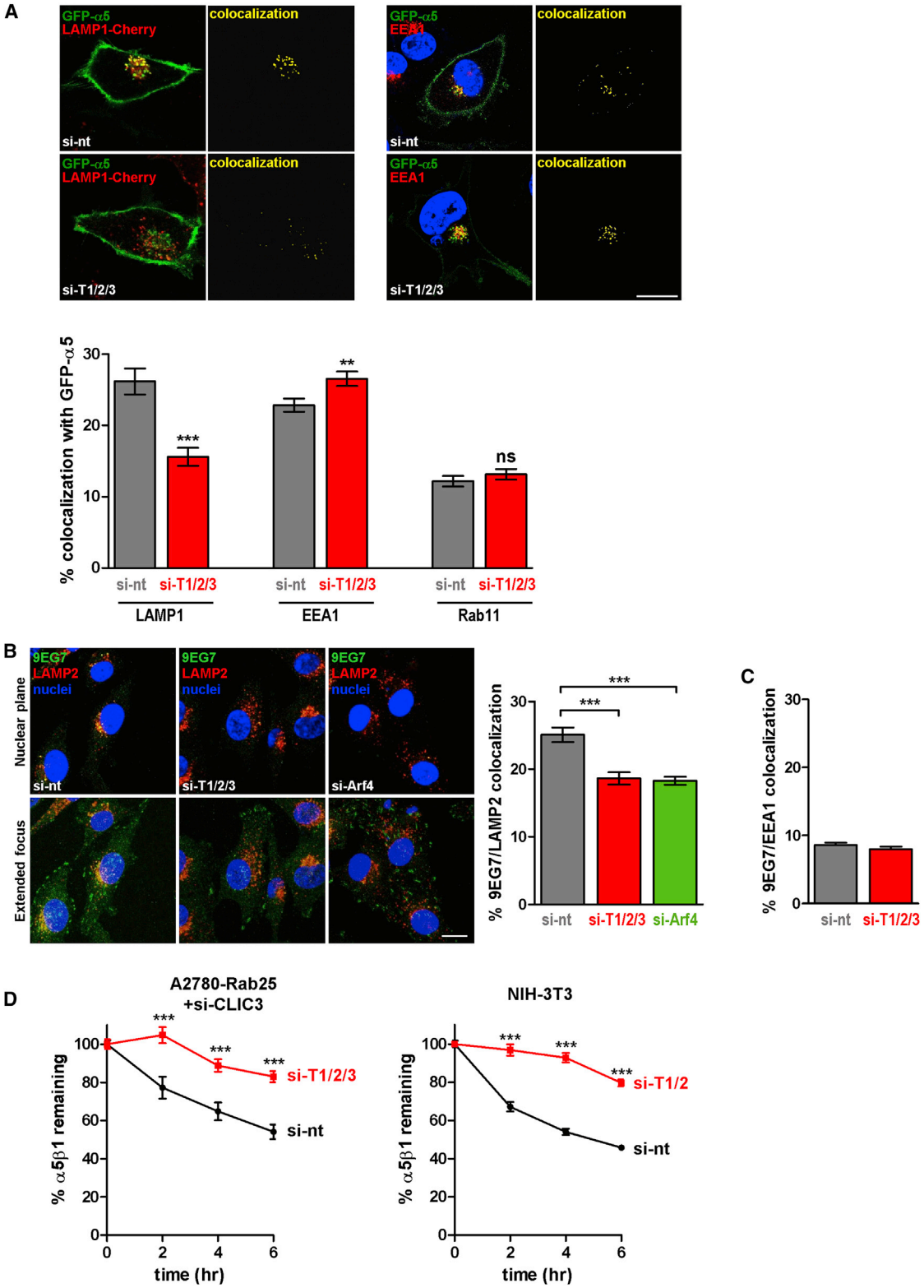

Figure 5. The Tensin/Arf4 Internalization Pathway Targets α5β1 to Lysosomes

(A) A2780-Rab25 cells were transfected with GFP-α5 (green) and LAMP1-cherry (red) or Cherry-Rab11a (red) in combination siRNAs targeting tensins-1, -2, and -3 (si-T1/2/3) or nontargeting control (si-nt) and allowed to adhere as for Figure 1E. Cells were fixed, stained for EEA1 and DAPI (as indicated), and imaged by

(legend continued on next page)

Tensin-1 Is Required for Invasion and Predicts Metastasis and Poor Survival in Pancreatic Ductal Adenocarcinoma

Rab25 expression increased invasiveness of A2780 cells into fibronectin-supplemented Matrigel plugs (Figure 7A) in a way that was dependent on α5β1 (data not shown). Consistently, Rab25 promoted extension of invasive pseudopods at the front of cells moving through 3D cell-derived matrix, and this was associated with a large increase in migratory persistence (Figure 7B). Knockdown of tensins-1, -2, and -3, individually or in combination, opposed Rab25's ability to drive migratory persistence and pseudopod extension in 3D cell-derived matrix and inhibited invasiveness through Matrigel (Figures 7A and 7B). By contrast, tensin knockdown did not affect migratory persistence or pseudopod length in cells that do not express Rab25 (Figure 7B).

Given the requirement for tensins in the Rab25-dependent internalization step, which feeds active integrins into the CLIC3 recycling pathway, we looked at the relationship between tensins and disease outcome in pancreatic adenocarcinoma. High tensin-1 (but not tensins-2, -3, or -4) expression was associated with shorter survival independent of tumor stage, lymph node spread, venous invasion, tumor size, and resection margin involvement (hazard ratio, 2.54; 95% CI, 1.13–5.69; $p = 0.024$). In univariate survival analysis, high levels of tensin-1 mRNA was associated with significantly decreased survival following tumor resection (Figure 7C). Upon analysis of the interaction between tensin-1 and CLIC3 in univariate survival analysis, we found that patients with tumors displaying low levels of both CLIC3 and tensin-1 mRNA had the best disease outcome (median survival of 55 months), and those tumors with high levels of both these transcripts were the most aggressive (median survival of 13.4 months) (Figure 7D). These data indicate that tensin, which regulates the endocytosis of active α5β1 integrins, is required for the invasiveness of cancer cells and indicate the likelihood that this integrin trafficking pathway contributes to invasion and metastasis in vivo.

DISCUSSION

In this paper, we have shown that, in Rab25-expressing cells, α5β1 integrins leave focal adhesions in the cell periphery to be translocated centripetally to a zone under the nucleus, and that the heterodimers must associate with tensin's PTB domain to undertake this journey. Upon reaching the subnuclear zone, ligand-engaged integrins are removed from the cell surface by endocytosis and transported to late endosomes/lysosomes. Because the forces that move α5β1 from peripheral focal adhesions toward the cell center are capable of generating the tension necessary to expose cryptic self-association sites in fibronectin, this movement is thought to contribute to generation of fibronectin fibrils (Pankov et al., 2000). Our data suggest an integrin translocator, which is initiated at one end by recruitment of α5β1 to focal adhesions, and terminated at the other by Arf4-dependent endocytosis. Thus, by dictating the time that α5β1 heterodimers spend stretching and remodeling fibronectin, tensin and Arf4 are likely to be key factors in defining the characteristics of ECM deposition. Endocytosis is thought to be necessary for proper assembly of fibronectin and collagen-containing ECM (Shi and Sottile, 2008), and our data provide a spatiotemporal framework for how this might be coordinated. Furthermore, coordination of centripetal integrin translocation and endocytosis may be influenced not only by Rab25, but also by the nutrient status of the cells via regulation of mTORC1. Indeed, in situations where mTORC1 is inhibited, tensin-dependent recruitment of integrins to subnuclear adhesions and their endocytosis from this region is strongly promoted, thus suggesting a mechanistic basis for coordination of ECM deposition and uptake with energy metabolism.

Many proteins interact with integrin tails in a mutually exclusive way, and the progression of integrins from one compartment to another may be accompanied by swapping of one interacting protein for another. β1 integrin's membrane distal NPxY binds to kindlin at the plasma membrane, but this site is occupied by SNX17 when the integrin moves to early endosomes (Böttcher et al., 2012). Likewise, the membrane proximal region of α5's tail is associated with Rab21 in early endosomes, but with p120RacGAP as the integrin moves to the recycling compartment—and these workers postulated that the relative affinities of these protein-protein interactions may generate unidirectionality of integrin transport (Mai et al., 2011). In A2780 cells, fibrillar adhesions are rich in tensin-1 (but not Rab25), and α5β1 internalization from these structures requires tensin's PTB domain to be capable of binding to the β1 integrin cytotail. By contrast, late endosomes that visit fibrillar adhesions to receive their integrin cargo are rich in Rab25, but do not contain tensin-1. Both Rab25 and tensin-1 associate with the β1 integrin cytodomain in a way that is likely mutually exclusive (data not shown), and it is possible that a swap of allegiance from tensin to Rab25 favors integrin delivery to late endosomes. Indeed, expression

confocal microscopy. The images displayed are confocal slices across the plane of the nucleus. Scale bar, 20 μm. ImageJ was used to quantify colocalization as indicated in the lower panel. This is expressed as the proportion of the intracellular compartment marker (red) that colocalizes with integrin (green), i.e., yellow pixels expressed as a fraction of red pixels. Values extracted from these analyses are mean ± SEM from three independent experiments; $^{**}p < 0.01$; $^{***}p < 0.001$, Mann-Whitney test.

(B and C) A2780-Rab25 cells were transfected with siRNAs targeting tensins-1, -2, and -3 (si-T1/2/3), Arf4 (si-Arf4), or nontargeting control (si-nt). Cells were allowed to adhere to glass-bottomed dishes coated with fibronectin (25 μg/ml) for 16 hr and were then fixed, stained for active β1 integrin (9EG7; green), LAMP2 (red, B) or EEA1 (C), and nuclei (blue), and imaged by confocal microscopy. The images displayed are confocal slices across the plane of the nucleus (top panels) and extended focus projections (bottom panels). Scale bar, 20 μm. Colocalization was quantified as for (A). Values are mean ± SEM from three independent experiments; $^{***}p < 0.001$, ANOVA test.

(D) A2780-Rab25 cells were transfected with siRNAs targeting CLIC3 in combination with those targeting tensins-1, -2, and -3 (si-T1/2/3) or nontargeting control (si-nt). NIH 3T3 fibroblasts were transfected with siRNAs targeting tensins-1 and -2 (si-T1/2) or nontargeting control (si-nt). Cells were surface-labeled with 0.13 mg/ml NHS-S-S-Biotin at 4°C and then warmed to 37°C in the presence of fibronectin for the indicated times. The proportion of α5β1 remaining was then determined using capture-ELISA. $^{***}p < 0.001$, ANOVA test.

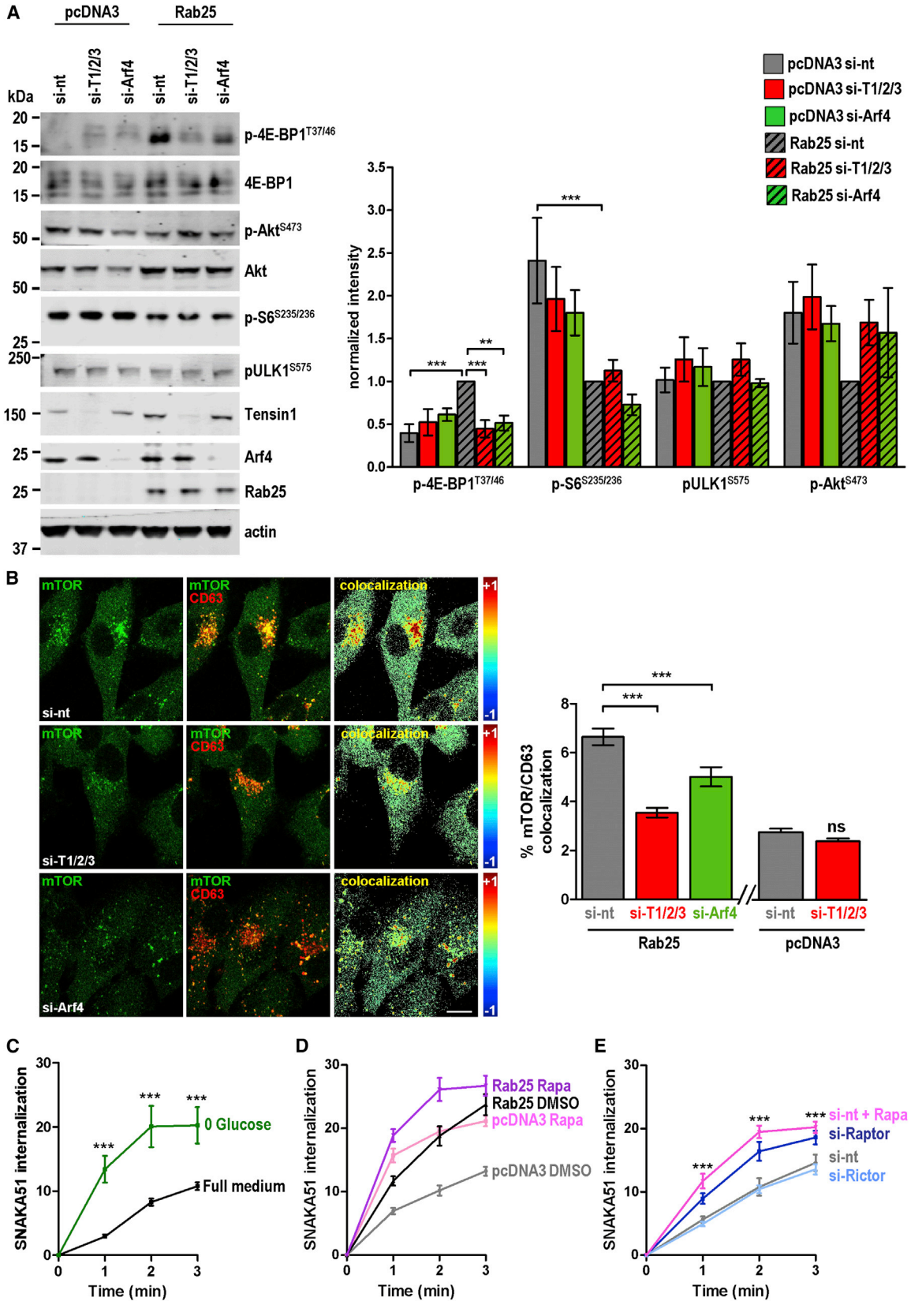

(legend on next page)

of Rab25 mutants that are incapable of associating with β1 integrin disturbs fibrillar adhesion morphology in A2780 cells (data not shown) indicating a requirement for integrin-Rab25 association in internalization of SNAKA51-positive α5β1. However, fibroblasts (including NIH 3T3s) do not express Rab25 indicating that this function may be fulfilled by another late endosomal protein with the capacity to displace tensin from the β1 cytotail, and further investigation will be necessary to substantiate this view. Furthermore, some physical force may be required to facilitate endocytosis of bulky integrin-ligand complexes. Our findings that endocytosis of ligand-engaged integrin requires both physical association with the actin-binding protein, tensin, and activity of the actin nucleating SCAR/WAVE complex is consistent with a need for actin polymerization to help drag integrin-ligand complexes into endosomes.

Antibody-chase experiments indicate that α5β1 can move from the cell surface to the recycling compartment via early endosomes (Roberts et al., 2001), and more recently the potential for α5β1 integrins to progress from early to late endosomes has been highlighted by studies indicating that SNX17 must associate with the β1 cytodomain to prevent the (presumably) default transport of α5β1 from early endosomes to lysosomes (Böttcher et al., 2012; Steinberg et al., 2012). However, receptors can exchange bidirectionally between lysosomes and the plasma membrane without passing through the earlier endosomal pathway (Lippincott-Schwartz and Fambrough, 1987), and recently we have shown that α5β1 can recycle directly from late endosomes/lysosomes to the cell surface (Dozynkiewicz et al., 2012). These data indicate the probability that exchange of material between late endosomes/lysosomes and the cell surface is bidirectional. Moreover, a recent study indicates that tubular connections form between late endosomal-type compartments and the plasma membrane that guide delivery of the transmembrane matrix metalloprotease, MT1-MMP to the cell surface in the subnuclear region (Monteiro et al., 2013), and we feel that it is likely that ECM proteolysis resulting from such exocytic events may be coordinated with Arf4-dependent endocytosis of ligand-engaged integrins from the same cellular region.

Blockade of internalization from fibrillar adhesions significantly increases the α5β1 content of early endosomes, indicating that when this pathway is blocked more integrin is available to follow endocytic routes that proceed via early endosomes. Taken together, these data indicate that ligand-occupied α5β1 heterodimers are internalized and recycled via a pathway that is morphologically distinct from the one that handles unoccupied integrins. The functions of these two pathways are likely to be different. Thus, pathways involving triage in early endosomes act to coordinate integrin and RTK (EGFR, cMET, and VEGFR2) trafficking and signaling (Caswell et al., 2009) and to implement integrin quality control by removing damaged heterodimers from the cell surface, as suggested by Böttcher et al. (2012). Conversely, transfer of ligand-occupied α5β1 from fibrillar adhesions to late endosomes supports central location of lysosomes and recruitment of mTOR to this subcellular region. Moreover, it is important to note that inhibition of mTOR promotes ligand-engaged integrin endocytosis indicating that the relationship between ECM internalization and mTOR signaling is governed by positive feedback.

Macropinocytosis of a serum protein (albumin) has been shown to generate a supply of amino acids necessary to sustain tumor cell bioenergetics (Commisso et al., 2013). The ECM is a potentially rich source of energy and building blocks in the form of amino acids and sugars, and our data indicate that tensin and Arf4 can support nutrient signaling via endocytosis of the ECM. Furthermore, we have previously shown that the late endosomal/lysosomal protein, CLIC3 acts to protect lysosomally targeted α5β1 from degradation and thus promote integrin recycling to the plasma membrane to drive invasion and metastasis (Dozynkiewicz et al., 2012). Our current study extends these observations by showing not only that tensin is connected with invasive migration and with metastasis in poorly vascularized tumors (such as pancreatic cancer), but also that the tensin-dependent route that delivers integrins to a proinvasive recycling pathway is strongly activated by nutrient depletion. Thus, our data indicate that low nutrient status of certain tumors may, by activating integrin trafficking, contribute to invasion and metastasis, and we provide mechanistic insights into how this might occur.

EXPERIMENTAL PROCEDURES

For a full description of the methods, please refer to Supplemental Experimental Procedures.

Cell Imaging, Photoactivation and Inverted Invasion Assays

Cells were seeded onto glass-bottomed 3.5 cm plates coated with fibronectin and imaged with a 64× objective of an inverted confocal microscope (Fluoview FV1000, Olympus) in an atmosphere of 5% CO_2 at 37°C. For TIRF, cells were imaged using a Plan Apo TIRF 100× objective, numerical aperture = 1.45, and a Nikon Eclipse Ti inverted microscope. Photoactivation of paGFP-α5 integrin in TIRF was with a pulse of 405 nm laser light. Colocalization quantification was performed using ImageJ software, where the confocal images underwent two rounds of local contrast enhancement (image blurring, subtraction of the blurred image, and subsequent contrast enhancement) and threshold adjustment. The number of yellow pixels was then expressed as a percentage of

Figure 6. Tensin and Arf4 Control Lysosomal Recruitment and Activation of mTOR

(A and B) A2780-pcDNA3 and A2780-Rab25 cells were transfected with siRNAs targeting tensins-1, -2, and -3 (si-T1/2/3), Arf4 (si-Arf4), or nontargeting control (si-nt) and incubated in RPMI containing 10% serum for 48 hr without replenishing the medium and then either lysed for western blot detection of mTOR substrates using the indicated phosphospecific antibodies and quantified using Li-Cor Odyssey software (A) or fixed for immunofluorescence visualization of mTOR (green) and CD63 (red) (B). The pixel-by-pixel colocalization of mTOR with CD63 was determined using an algorithm in which areas of high colocalization are depicted by the red pseudocolor, and pixels in which the mTOR or CD63 were present but not colocalized with one another are represented by the blue pseudocolor. Scale bar, 20 μm. Values extracted from these analyses are the mean ± SEM from three independent experiments. ***$p < 0.001$, **$p < 0.01$, ANOVA test.

(C–E) A2780-pcDNA3 or A2780-Rab25 cells were transfected with siRNAs targeting Rictor (si-Rict), Raptor (si-Rapt), or nontargeting control (si-nt), or treated with rapamycin (1 μM) or DMSO vehicle for 2 hr, or glucose-starved (0 glucose) for 2 hr. Values are mean ± SEM from three independent experiments. In the left panel, ***$p < 0.001$ ANOVA test, in the middle panel the pcDNA3 Rapa. (pink) values are significantly different from the pcDNA3 DMSO ones, $p < 0.001$, ANOVA test. In the right panel, the si-Raptor (dark blue) values are significantly different from the si-nt ones, $p < 0.001$, ANOVA test.

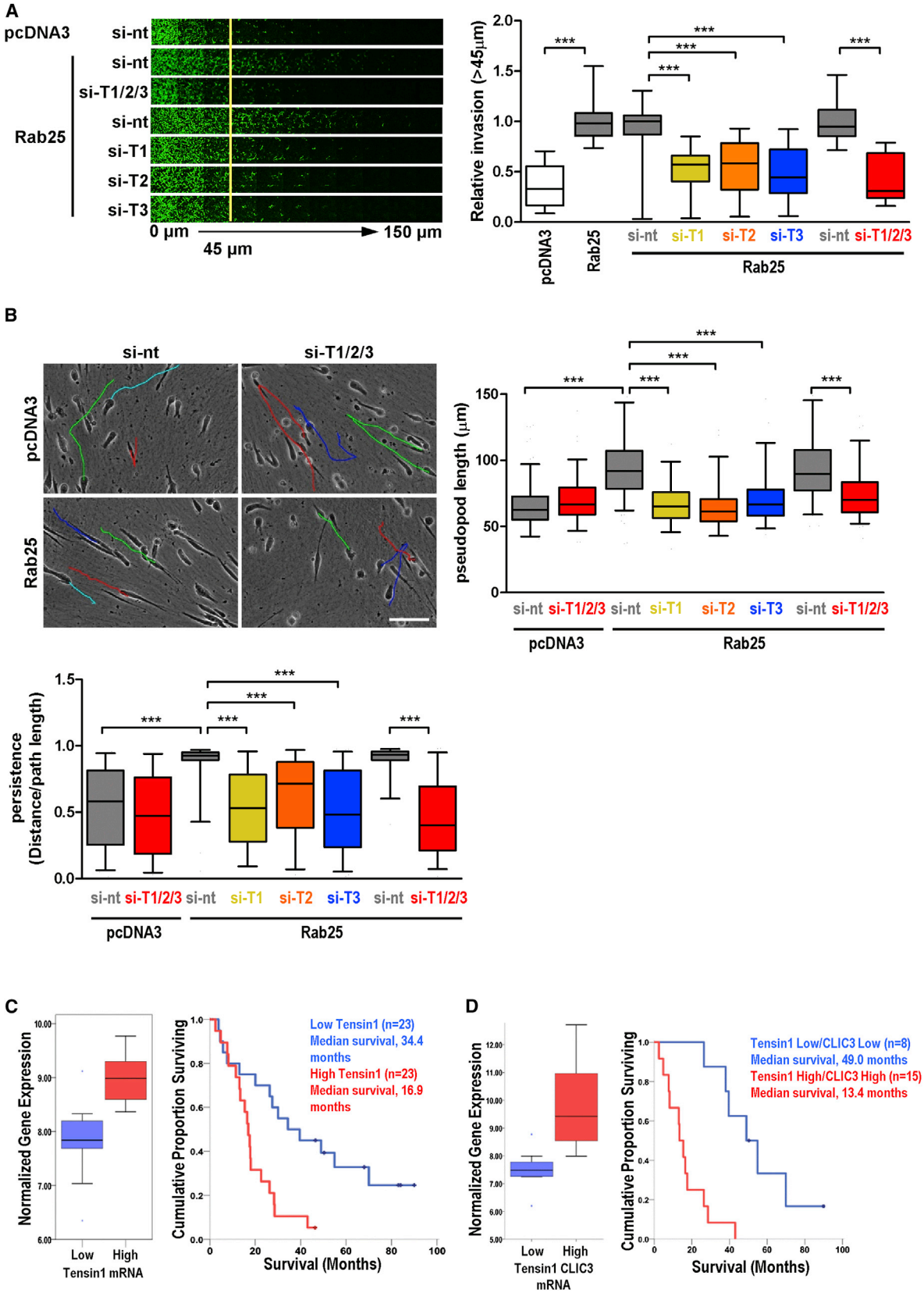

(legend on next page)

pixels in the red channel. Inverted (Hennigan et al., 1994) invasion assays were performed as described previously.

Internalization Assays

Integrin internalization assays were performed as described previously in Roberts et al. (2001). Internalization was allowed to proceed at 37°C in the presence of 0.6 mM primaquine. The following antibodies were used for capture-ELISA; clone VC5 (Pharmingen) for total α5β1 (human), SNAKA51, which was generously donated by Martin Humphries (University of Manchester, UK), and anti-CD71 (Pharmingen) for the TfnR.

SUPPLEMENTAL INFORMATION

Supplemental Information includes Supplemental Experimental Procedures, seven figures, and six movies and can be found with this article online at http://dx.doi.org/10.1016/j.celrep.2014.12.037.

ACKNOWLEDGMENTS

The work at the Beatson Institute in J.C.N.'s lab is funded by Cancer Research UK and the Breast Cancer Campaign. E.R. is funded by the West of Scotland Women's Bowling Association. Many thanks to Martin Humphries and Kath Clark for the generous gift of SNAKA51 antibody, to Ken Yamada for tensin constructs, and to Donna Webb for GFP-α5.

Received: April 7, 2014
Revised: November 21, 2014
Accepted: December 16, 2014
Published: January 15, 2015

REFERENCES

Arjonen, A., Alanko, J., Veltel, S., and Ivaska, J. (2012). Distinct recycling of active and inactive beta1 integrins. Traffic *13*, 610–625.

Böttcher, R.T., Stremmel, C., Meves, A., Meyer, H., Widmaier, M., Tseng, H.Y., and Fässler, R. (2012). Sorting nexin 17 prevents lysosomal degradation of β1 integrins by binding to the β1-integrin tail. Nat. Cell Biol. *14*, 584–592.

Caswell, P.T., and Norman, J.C. (2006). Integrin trafficking and the control of cell migration. Traffic *7*, 14–21.

Caswell, P.T., Chan, M., Lindsay, A.J., McCaffrey, M.W., Boettiger, D., and Norman, J.C. (2008). Rab-coupling protein coordinates recycling of alpha5beta1 integrin and EGFR1 to promote cell migration in 3D microenvironments. J. Cell Biol. *183*, 143–155.

Caswell, P.T., Vadrevu, S., and Norman, J.C. (2009). Integrins: masters and slaves of endocytic transport. Nat. Rev. Mol. Cell Biol. *10*, 843–853.

Chao, W.T., and Kunz, J. (2009). Focal adhesion disassembly requires clathrin-dependent endocytosis of integrins. FEBS Lett. *583*, 1337–1343.

Clark, K., Pankov, R., Travis, M.A., Askari, J.A., Mould, A.P., Craig, S.E., Newham, P., Yamada, K.M., and Humphries, M.J. (2005). A specific alpha5beta1-integrin conformation promotes directional integrin translocation and fibronectin matrix formation. J. Cell Sci. *118*, 291–300.

Clark, K., Howe, J.D., Pullar, C.E., Green, J.A., Artym, V.V., Yamada, K.M., and Critchley, D.R. (2010). Tensin 2 modulates cell contractility in 3D collagen gels through the RhoGAP DLC1. J. Cell. Biochem. *109*, 808–817.

Commisso, C., Davidson, S.M., Soydaner-Azeloglu, R.G., Parker, S.J., Kamphorst, J.J., Hackett, S., Grabocka, E., Nofal, M., Drebin, J.A., Thompson, C.B., et al. (2013). Macropinocytosis of protein is an amino acid supply route in Ras-transformed cells. Nature *497*, 633–637.

D'Souza-Schorey, C., and Chavrier, P. (2006). ARF proteins: roles in membrane traffic and beyond. Nat. Rev. Mol. Cell Biol. *7*, 347–358.

Dozynkiewicz, M.A., Jamieson, N.B., Macpherson, I., Grindlay, J., van den Berghe, P.V., von Thun, A., Morton, J.P., Gourley, C., Timpson, P., Nixon, C., et al. (2012). Rab25 and CLIC3 collaborate to promote integrin recycling from late endosomes/lysosomes and drive cancer progression. Dev. Cell *22*, 131–145.

Efeyan, A., Zoncu, R., and Sabatini, D.M. (2012). Amino acids and mTORC1: from lysosomes to disease. Trends Mol. Med. *18*, 524–533.

Ezratty, E.J., Bertaux, C., Marcantonio, E.E., and Gundersen, G.G. (2009). Clathrin mediates integrin endocytosis for focal adhesion disassembly in migrating cells. J. Cell Biol. *187*, 733–747.

Gu, Z., Noss, E.H., Hsu, V.W., and Brenner, M.B. (2011). Integrins traffic rapidly via circular dorsal ruffles and macropinocytosis during stimulated cell migration. J. Cell Biol. *193*, 61–70.

Hennigan, R.F., Hawker, K.L., and Ozanne, B.W. (1994). Fos-transformation activates genes associated with invasion. Oncogene *9*, 3591–3600.

Howes, M.T., Kirkham, M., Riches, J., Cortese, K., Walser, P.J., Simpson, F., Hill, M.M., Jones, A., Lundmark, R., Lindsay, M.R., et al. (2010). Clathrin-independent carriers form a high capacity endocytic sorting system at the leading edge of migrating cells. J. Cell Biol. *190*, 675–691.

Korolchuk, V.I., Saiki, S., Lichtenberg, M., Siddiqi, F.H., Roberts, E.A., Imarisio, S., Jahreiss, L., Sarkar, S., Futter, M., Menzies, F.M., et al. (2011). Lysosomal positioning coordinates cellular nutrient responses. Nat. Cell Biol. *13*, 453–460.

Kumari, S., and Mayor, S. (2008). ARF1 is directly involved in dynamin-independent endocytosis. Nat. Cell Biol. *10*, 30–41.

Lee, J.W., and Juliano, R.L. (2000). alpha5beta1 integrin protects intestinal epithelial cells from apoptosis through a phosphatidylinositol 3-kinase and protein kinase B-dependent pathway. Mol. Biol. Cell *11*, 1973–1987.

Lippincott-Schwartz, J., and Fambrough, D.M. (1987). Cycling of the integral membrane glycoprotein, LEP100, between plasma membrane and lysosomes: kinetic and morphological analysis. Cell *49*, 669–677.

Lobert, V.H., and Stenmark, H. (2012). The ESCRT machinery mediates polarization of fibroblasts through regulation of myosin light chain. J. Cell Sci. *125*, 29–36.

Lobert, V.H., Brech, A., Pedersen, N.M., Wesche, J., Oppelt, A., Malerød, L., and Stenmark, H. (2010). Ubiquitination of alpha 5 beta 1 integrin controls

Figure 7. Tensin Is Required for Invasiveness in 3D Microenvironments and Dictates Poor Patient Survival in Pancreatic Adenocarcinoma

(A and B) A2780-pcDNA3 and A2780-Rab25 cells were transfected with siRNAs targeting tensins-1 (si-T1), -2 (si-T2), or -3 (si-T3) either alone or in combination (si-T1/2/3). Invasiveness of transfected cells into fibronectin-supplemented (25 μg/ml) Matrigel was determined using an inverted invasion assay. Invasion is expressed as the proportion of cells that migrate further than 45 μm. Data are represented as box and whiskers plots (min to max); ***$p < 0.001$ ANOVA test (A). For (B), cells were plated onto fibroblast cell-derived matrix. Images were captured every 10 min over a 16 hr period, and movies were generated from these. The migratory persistence and the invasive pseudopod length (defined as the distance between the center of the nucleus and the cell front with respect to the direction of migration) were measured using ImageJ. Scale bar, 100 μm. Data are represented as box and whiskers plots (whiskers: 5–95 percentile); ***$p < 0.001$; ANOVA test.

(C) Box plot illustrating stratification of pancreatic adenocarcinoma patients into low and high tensin-1 expressors based on normalized mean gene expression. Kaplan-Meier analysis comparing the survival outcome of patients with tumors expressing high levels of tensin-1 mRNA (red; n = 23) with those expressing lower tensin-1 levels (blue; n = 23) following tumor resection ($p = 0.003$).

(D) Pancreatic adenocarcinoma were analyzed as for (C), but with the tumors being grouped into those that express high levels of both tensin-1 and CLIC3 (red; n = 15) compared with those expressing low levels of both genes (blue; n = 8) $p < 0.0001$ for the Kaplan-Meier analysis.

fibroblast migration through lysosomal degradation of fibronectin-integrin complexes. Dev. Cell *19*, 148–159.

Mai, A., Veltel, S., Pellinen, T., Padzik, A., Coffey, E., Marjomäki, V., and Ivaska, J. (2011). Competitive binding of Rab21 and p120RasGAP to integrins regulates receptor traffic and migration. J. Cell Biol. *194*, 291–306.

Margadant, C., Kreft, M., de Groot, D.J., Norman, J.C., and Sonnenberg, A. (2012). Distinct roles of talin and kindlin in regulating integrin alpha5beta1 function and trafficking. Curr. Biol *22*, 1554–1563.

McCleverty, C.J., Lin, D.C., and Liddington, R.C. (2007). Structure of the PTB domain of tensin1 and a model for its recruitment to fibrillar adhesions. Protein Sci. *16*, 1223–1229.

Monteiro, P., Rossé, C., Castro-Castro, A., Irondelle, M., Lagoutte, E., Paul-Gilloteaux, P., Desnos, C., Formstecher, E., Darchen, F., Perrais, D., et al. (2013). Endosomal WASH and exocyst complexes control exocytosis of MT1-MMP at invadopodia. J. Cell Biol. *203*, 1063–1079.

Muller, P.A., Caswell, P.T., Doyle, B., Iwanicki, M.P., Tan, E.H., Karim, S., Lukashchuk, N., Gillespie, D.A., Ludwig, R.L., Gosselin, P., et al. (2009). Mutant p53 drives invasion by promoting integrin recycling. Cell *139*, 1327–1341.

Muller, P.A., Trinidad, A.G., Timpson, P., Morton, J.P., Zanivan, S., van den Berghe, P.V., Nixon, C., Karim, S.A., Caswell, P.T., Noll, J.E., et al. (2012). Mutant p53 enhances MET trafficking and signalling to drive cell scattering and invasion. Oncogene.

Pankov, R., Cukierman, E., Katz, B.Z., Matsumoto, K., Lin, D.C., Lin, S., Hahn, C., and Yamada, K.M. (2000). Integrin dynamics and matrix assembly: tensin-dependent translocation of alpha(5)beta(1) integrins promotes early fibronectin fibrillogenesis. J. Cell Biol. *148*, 1075–1090.

Pellinen, T., and Ivaska, J. (2006). Integrin traffic. J. Cell Sci. *119*, 3723–3731.

Pellinen, T., Tuomi, S., Arjonen, A., Wolf, M., Edgren, H., Meyer, H., Grosse, R., Kitzing, T., Rantala, J.K., Kallioniemi, O., et al. (2008). Integrin trafficking regulated by Rab21 is necessary for cytokinesis. Dev. Cell *15*, 371–385.

Rainero, E., and Norman, J.C. (2013). Late endosomal and lysosomal trafficking during integrin-mediated cell migration and invasion: Cell matrix receptors are trafficked through the late endosomal pathway in a way that dictates how cells migrate. BioEssays *35*, 523–532.

Roberts, M., Barry, S., Woods, A., van der Sluijs, P., and Norman, J. (2001). PDGF-regulated rab4-dependent recycling of alphavbeta3 integrin from early endosomes is necessary for cell adhesion and spreading. Curr. Biol. *11*, 1392–1402.

Shi, F., and Sottile, J. (2008). Caveolin-1-dependent beta1 integrin endocytosis is a critical regulator of fibronectin turnover. J. Cell Sci. *121*, 2360–2371.

Steinberg, F., Heesom, K.J., Bass, M.D., and Cullen, P.J. (2012). SNX17 protects integrins from degradation by sorting between lysosomal and recycling pathways. J. Cell Biol. *197*, 219–230.

Tang, H., Li, A., Bi, J., Veltman, D.M., Zech, T., Spence, H.J., Yu, X., Timpson, P., Insall, R.H., Frame, M.C., et al. (2013). Loss of Scar/WAVE complex promotes N-WASP- and FAK-dependent invasion. Curr. Biol. *23*, 107–117.

Teckchandani, A., Toida, N., Goodchild, J., Henderson, C., Watts, J., Wollscheid, B., and Cooper, J.A. (2009). Quantitative proteomics identifies a Dab2/integrin module regulating cell migration. J. Cell Biol. *186*, 99–111.

Valdembri, D., Caswell, P.T., Anderson, K.I., Schwarz, J.P., König, I., Astanina, E., Caccavari, F., Norman, J.C., Humphries, M.J., Bussolino, F., and Serini, G. (2009). Neuropilin-1/GIPC1 signaling regulates alpha5beta1 integrin traffic and function in endothelial cells. PLoS Biol. *7*, e25.